



OUT-OF-PLANE SHAKE TABLE TESTING OF URM WALLS WITH PARAPETS AND WOOD DIAPHRAGMS

Juan ALEMAN¹, Gilberto MOSQUEDA² and Andrew WHITTAKER³

ABSTRACT

Although the vulnerability of unreinforced masonry walls to out-of-plane damage and collapse has been observed many times in past earthquakes, there is little experimental data with which to develop and validate robust numerical models.

This paper discusses shake table testing of two full-scale multi-wythe unreinforced masonry walls with parapets and wood diaphragms subjected to out-of-plane loading. The walls were built with materials typical of late 19th-early 20th Century construction in New York City and were intended to simulate a central portion of a one-story URM building. The parapet and wall-to-diaphragm connection of one of the walls were conventionally strengthened with diagonal steel bracing and steel rods, respectively. The walls were subjected to a sequence of two sets of ground motions with increasing intensity: the 2011 Mineral Virginia earthquake and the 2011 Christchurch New Zealand earthquake. Both masonry walls sustained the Virginia earthquake having a PGA of 0.20 g with minor damage. However, collapse of the parapet and the connection between masonry walls and wood joist was observed when the specimens were subjected to the New Zealand earthquake with a PGA equals to 0.36g. The results of these tests provided valuable data and knowledge regarding the seismic behavior and vulnerability of masonry walls with parapets and flexible diaphragms. Further, information on the wall-to-diaphragm connection has been collected and will be used to judge the effectiveness of this retrofitting technique and to validate computer models to be used for seismic vulnerability assessments.

INTRODUCTION

The vulnerability of unreinforced masonry walls with parapets and flexible wood diaphragms to out-of-plane damage and collapse has been documented following many earthquakes. Common failures include parapets and chimneys falling to the ground and masonry walls collapsing due to failure of their connection to adjacent wood diaphragms. Experimental data on the seismic behavior of these critical structural components is scarce and the effectiveness of strengthened parapets and floor-to-wall connections has never been experimentally tested. Current stability limits for out-of-plane unreinforced masonry (URM) walls, as described in ASCE 41 (2006), are based on recommendations provided by the ABK experimental program (ABK 1984), which did not include URM walls with parapets and realistic connections. More recently, Krawinkler et al. (2012) developed fragility functions for parapets and chimneys based on a combination of engineering judgment, empirical data and sophisticated numerical models subjected to the ATC-63 far-field ground motion set, with a focus on masonry construction on the West Coast of the United States. The seismic vulnerability of URM

¹ Engineer, Arup, Los Angeles, USA, juan.aleman@arup.com

² Associate Professor, University of California, San Diego, USA, gmosqueda@ucsd.edu

³ Professor and Chair Director MCEER, University of Buffalo, New York, USA, awhittak@buffalo.edu

buildings with parapets and flexible diaphragms in regions of medium and low seismic hazard, similar to New York City (NYC), remains unexplored although it is expected to be high. There is a pressing need to obtain experimental data to verify and validate simplified numerical models that can be used by structural engineering practitioners to understand the most likely behavior and interaction between components of this complex, poorly-understood system.

The experiment testing described in this paper is part of a comprehensive study currently under way at the University at Buffalo. This study will develop and validate numerical models to be used for seismic vulnerability assessments of URM buildings in NYC. More detailed information can be found in Aleman (2014).

TEST SETUP

Wall specimens were selected to simulate a central portion of one-story URM buildings in NYC, as illustrated in Fig. 1. Two identical full-scale masonry walls were constructed on a shake table. The dimensions of the walls were approximately 6 feet in width, 14 feet in height and 1 foot thick. Similar dimensions have been used by Meisl et al. (2007) and Penner and Elwood (2012) in testing of out-of-plane URM walls. Data obtained from material identification tests previously conducted has been considered in selecting the properties of brick and mortar for the walls. Reclaimed bricks were laid out using an American Bond pattern. The mortar proportions were target to match a Type K mortar (1:3:10), but to improve workability during construction, a slightly stronger mortar was used. An adjustable steel base restraint was placed at the bottom of each wall, to prevent sliding but to allow free rotation. The configuration is illustrated in Fig. 2 and Fig. 3.

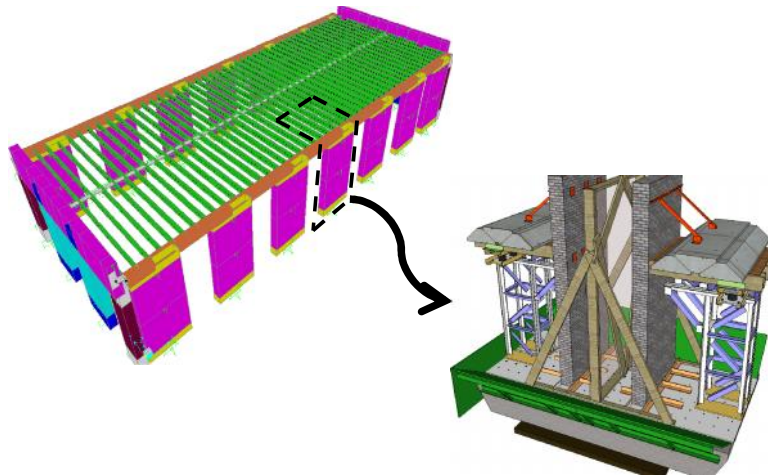


Figure 1. Design concept of wall specimens

Two standard retrofitting techniques were implemented in Wall 2, which is defined in Fig.2. These techniques are recommended in FEMAP547 (2006), but these procedures have a largely empirical basis and have not been tested in a laboratory, to the knowledge of the authors. The simplest way to prevent out-of-plane collapse of URM walls is to tie them to the floor using steel anchors. The next step to achieve Life Safety is to fix the parapets and the chimneys to the roof using steel braces. Structural details to incorporate those details in the specimen are presented in Fig.3.

Diaphragm flexibility was simulated using flexible low damping rubber (LDR) and stiff lead rubber (LRB) bearings isolators. Four LRB and four LDR were installed in Wall 1 and Wall 2, respectively. The isolators were bolted to the steel tower, as illustrated in Fig.3. The selection of the number and properties of the isolators are described in Aleman (2014). The physical properties of the isolators were obtained from previous experimental studies (Sanchez-Ferreira 2011).

Two rigid steel towers were used to support the wood floors and transfer the input acceleration from the base of the table to the top of the diaphragm without significant amplification. The elastic stiffness of each frame was about 3000 kip/in. Each frame had a total weight of 6 kips.

The wood floors were designed to support additional dead load and to provide a realistic connection between the masonry walls and the diaphragm. The dimensions were selected to match the width of the wall and to accommodate concrete blocks that provided additional floor mass. Each wood joist was placed at 16" inches. All boards and joist were constructed of Douglas Fir material. Typical 8d nails were used to connect the wood boards and joists. The wood diaphragms were constructed at the laboratory and then placed on top of each steel tower. The wood floors were bolted to steel angles, which in turn were welded to the base of each isolator. Three concrete blocks were placed on top of each wood floor. The average weight of each block was about 1 kip. The blocks were attached to the wood floors using standard 7/8" diameter bolts.

A safety frame was built in the middle of the shake table to prevent one wall from damaging the other. The frame was designed to resist the maximum impact load that could be generated by the mass of the wall if sliding out the joist pockets. Steel plates were placed around the shake table to prevent falling bricks from posing a hazard to the shaking table. The walls were tested simultaneously as described in the next section. Details of the test setup are provided in Aleman (2014).

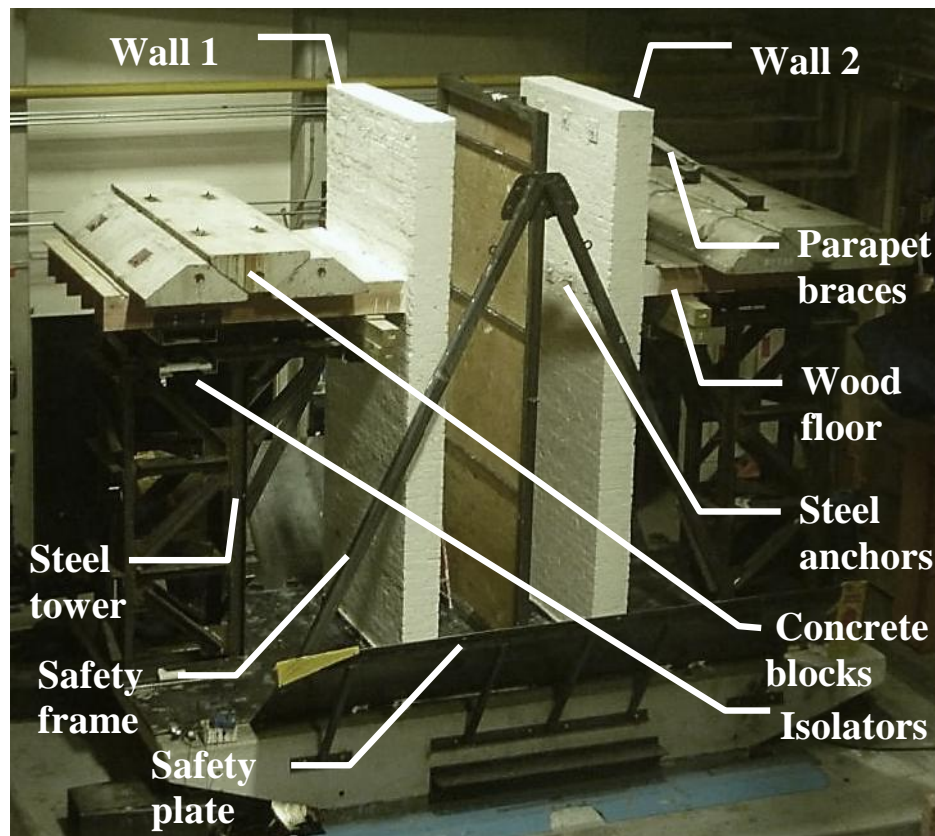


Figure 2. Wall specimens and key components of the test setup

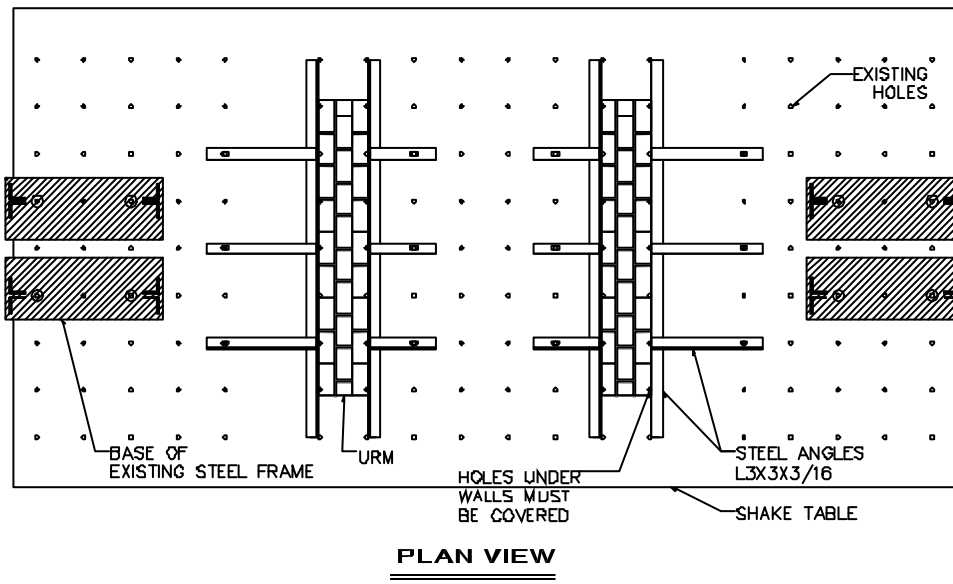
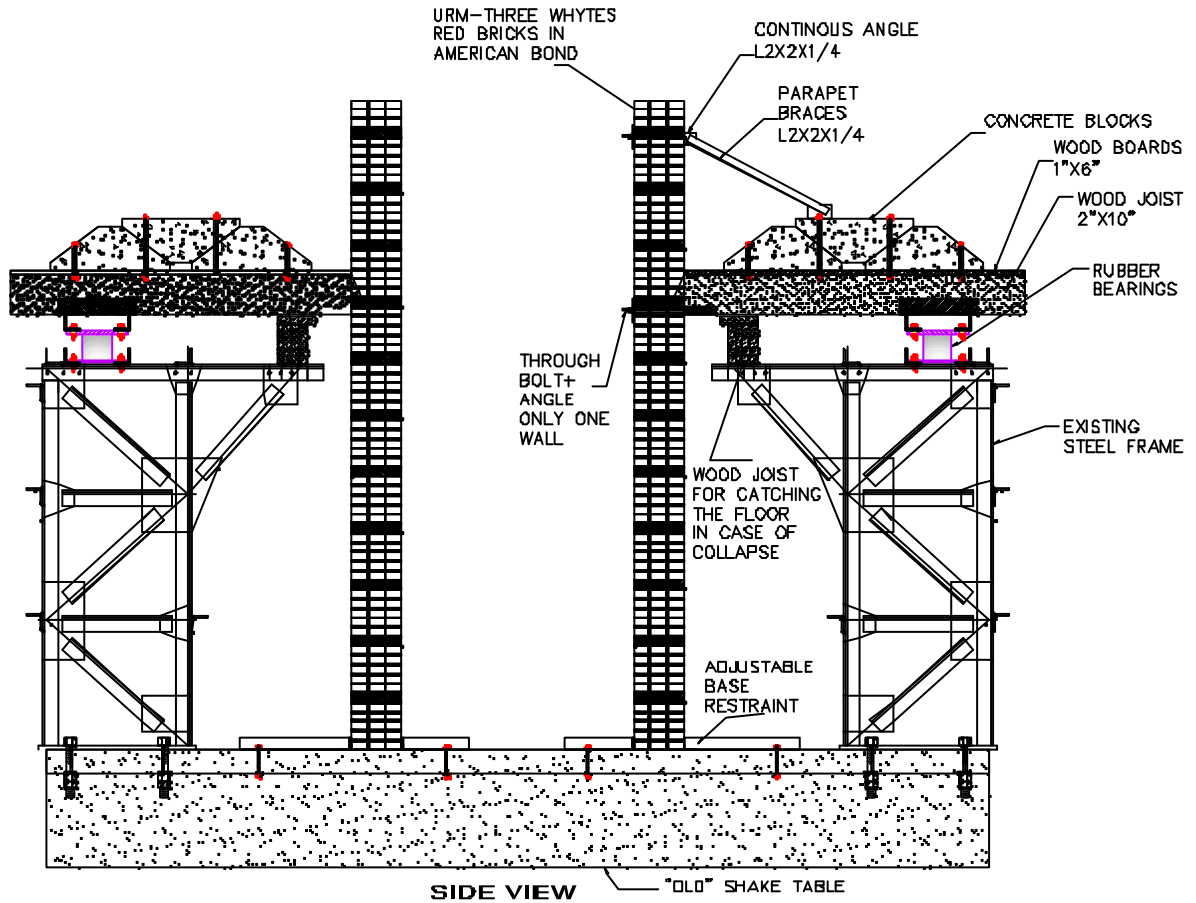


Figure 3. Structural plan view and elevation of test setup

TEST PROCEDURES

Two ground motions were used as input to the shake table, with one motion selected for its high frequency content and the other for its low frequency content. The short-period motion selected was recorded during the 23 August 2011 Mineral earthquake in Virginia, USA. The long-period motion selected was recorded during the 21 February 2011 earthquake in Christchurch, New Zealand. Response spectra of the two motions are shown in Fig. 4a, and Fig. 4b, respectively.

The ground motions were scaled up or down to match the MCE Response Spectrum for a site Class A located in New York City (coordinates 40.7724,-73.9670). The MCE Spectrum was obtained using the Hazard Tool provided at the USGS website. Fig. 4a also shows the MCE Response Spectrum.

The specimens were subjected to an increasing intensity sequence of nine dynamic tests until collapse. The loading protocol was designed to gradually introduce damage in the specimens. Only one component of each ground motion was applied in the X-direction or South-North direction. White-noise excitation with acceleration amplitude of 0.03g was applied first to the specimen to identify its dynamic properties. The testing sequence listed in Table 1 was followed thereafter. Note that for the Virginia Earthquake, the actual PGAs obtained during the tests were significant smaller than the target PGAs.

Table 1. Test Sequence followed for two-wall specimen

Earthquake/Input	Test No.	Target PGA (g)	Actual PGA (g)	Scale Factor	Target Hazard Level
White noise	1	0.03	0.03	n/a	n/a
	2	0.033	0.012	30%	Service Level
	3	0.11	0.05	100%	MCE Spectrum
Virginia_Reston (Mw=5.8, R=124.1 km)	4	0.16	0.07	150%	1.5 MCE Spectrum
	5	0.22	0.11	200%	2 MCE Spectrum
	6	0.32	0.20	300%	3 MCE Spectrum
	7	0.18	0.20	50%	MCE Spectrum
NZ_Hospital (Mw=6.3, R=10 km)	8	0.27	0.26	75%	1.5 MCE Spectrum
	9	0.36	0.36	100%	2 MCE Spectrum

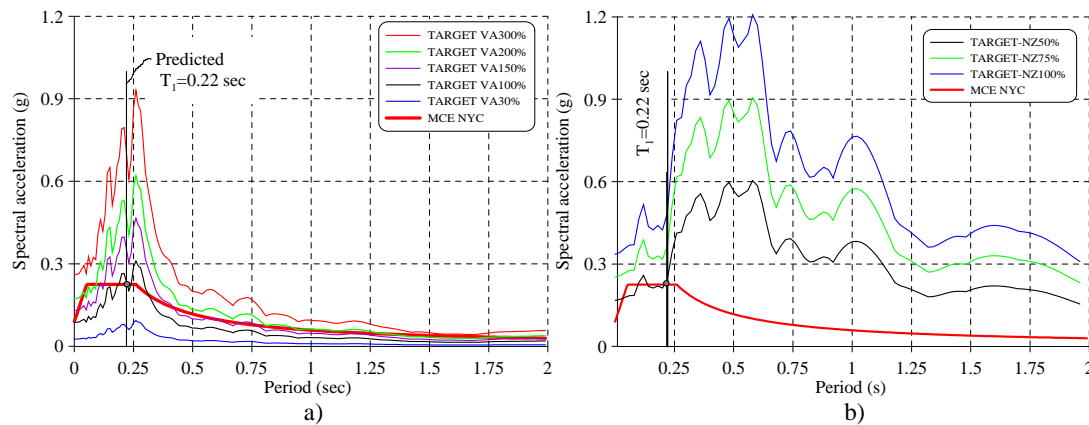


Figure 4. Scaled response spectra to match MCE in New York City of a) Virginia earthquake and b) New Zealand earthquake

TEST RESULTS FOR VIRGINIA_RESTON EARTHQUAKE

Peak values of relative displacement response at several locations in Wall 1 and Wall 2 are shown in Fig. 5a. A linear distribution of relative displacement over the height can be observed for all tests. Since the walls were free to rotate at the base, rigid body rocking around the base was the predominant behavior. The inertia generated in the masonry walls was insufficient to crack the walls. Moreover, no relative displacements were observed at the connection between the wood joist and the masonry wall.

Peak values of absolute acceleration response at several locations in Wall 1 and Wall 2 are shown in Fig. 6a. Constant acceleration profiles along the height of uncracked walls are expected when the wall is rigidly connected at the top and bottom, as discussed in Meisl et al. (2007). Nonetheless, for intensities VA150%, VA200% and VA300% a parabolic profile can be observed, revealing a strong influence of the parapet and the frequency content of the seismic input in the distribution of inertial forces in the wall.

Large relative displacement was observed at the top of the steel tower, as shown in Fig. 5b. This was due to a rigid body rotation at the base of the steel tower, which was connected to the most flexible part of the shake table. The flexibility of this part of the table affected the seismic response of the tower, as can also be seen in Figure 6, in which absolute accelerations decreased.

The influence of diaphragm stiffness can be seen in Fig. 5b and Fig. 6b. As expected, larger peak relative displacements of the isolators were observed in Wall 2. However, the absolute acceleration was slightly amplified at the diaphragm level (height=115 in), regardless of the type of isolator implemented and the rigid body rotation of the towers. The peak absolute accelerations are about the same in both specimens for a given simulation, demonstrating the effectiveness of using steel braces as a retrofitting technique to overall reduce seismic demands.

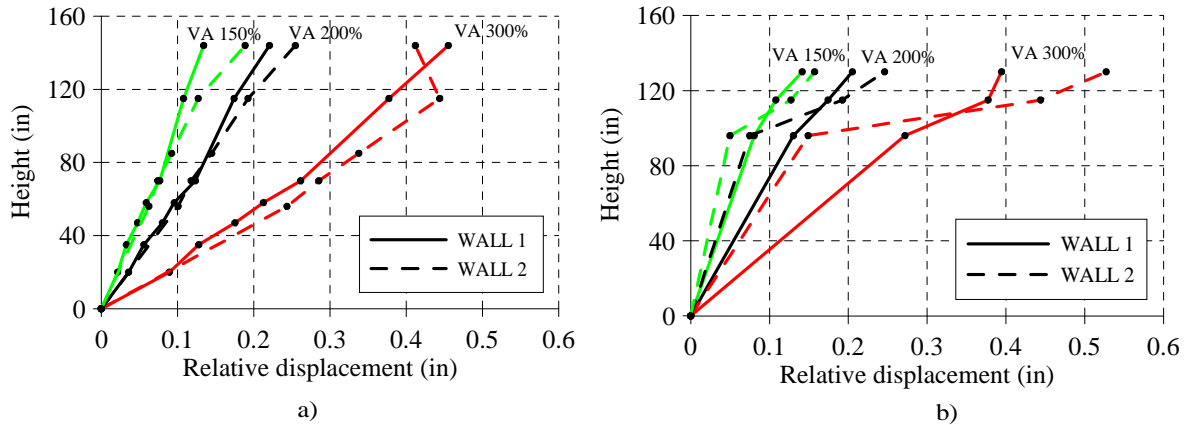


Figure 5. Peak relative displacement profile of Wall 1 and Wall 2 obtained for Virginia earthquake: a) masonry wall and b) steel tower and isolators

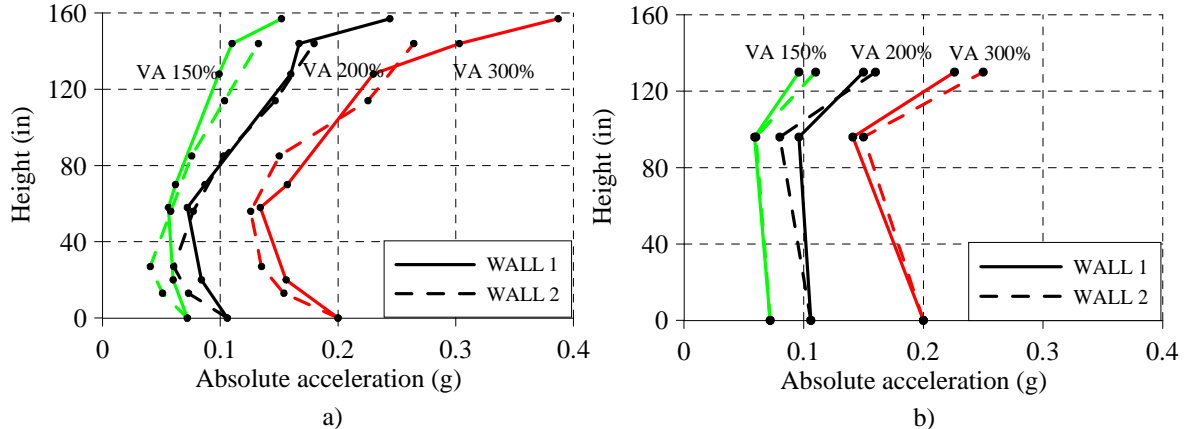


Figure 6. Peak absolute acceleration profiles of Wall 1 and Wall 2 at a) masonry wall and b) steel tower and isolators

TEST RESULTS FOR NZ_HOSPITAL EARTHQUAKE

Peak values of relative displacement response at several locations in Wall 1 are shown in Fig. 7a . A linear distribution along the height of the wall, up to the wood diaphragm level can be observed for intensity levels NZ50% and NZ75%. This linear distribution is attributed to the rigid body rocking motion at the base of the wall. The large peak relative displacement observed at the base of the parapets , with respect to the diaphragm level, it is due to cracking in this zone. From this figure, it is implied that the inertia generated in the masonry wall for these tests was enough to generate small cracks in the portion of the wall below the wood diaphragm. Also, no relative displacement is observed at the connection between the wood joist and the masonry wall.

Peak values of absolute acceleration response along the height of Wall 1 are shown in Fig. 8a. A linear profile of absolute accelerations can be seen for intensity levels NZ50% and NZ75%. For NZ100%, higher amplification can be seen at the parapet, due to rocking behavior at its base.

As in the Virginia Earthquake tests, a large relative displacement is also observed at the top of the steel tower, as shown in Fig.7b. The absolute acceleration was amplified at this level, as can also be seen in Fig.8b. Fig. 7b also shows a significant sliding between the concrete blocks and the wood floor.

Fig. 7a also shows peak values of relative displacement response in Wall 2. Different from Wall 1, a nonlinear distribution along the height of the specimen up to the wood diaphragm level can be observed for all intensity levels. This nonlinear distribution is attributed to cracking in the wall below the wood diaphragm. The large relative displacement observed for the parapet is also an indication of cracking. Also, Fig.7a shows that the peak displacement at the wood diaphragm is reduced after cracking of the portion of the wall beneath the parapet.

Peak values of absolute acceleration response along the height of Wall 2 are shown in Fig. 8a. A nonlinear profile of absolute accelerations was obtained for all intensity levels due to cracking at the mid-height of the wall between the wood floor and the base. Because of the relative large flexibility of the diaphragm, the absolute input acceleration was amplified at the wood diaphragm, steel tower, concrete blocks and parapet level, as illustrated in Fig. 8b.

Peak axial stresses in the steel anchors between wood joists for all intensity levels of NZ earthquake are shown in Fig. 9. As expected, the maximum stress increases with an increase in the intensity of the motion and the effect of wall failure. The axial stress in the central anchors was almost 2.5 higher than the axial stress in the edge anchors. This is because the tributary seismic mass is higher at the center of the wall.

Fig.10 shows the peak axial stresses in steel braces in Wall 2 for all shaking intensities involving the NZ earthquake. The non-uniform distribution of stresses indicates that one brace was attracting more seismic force than the other. This was due to a loose connection between the wall and one of the braces. As expected, the axial stress was well below the yielding limit.

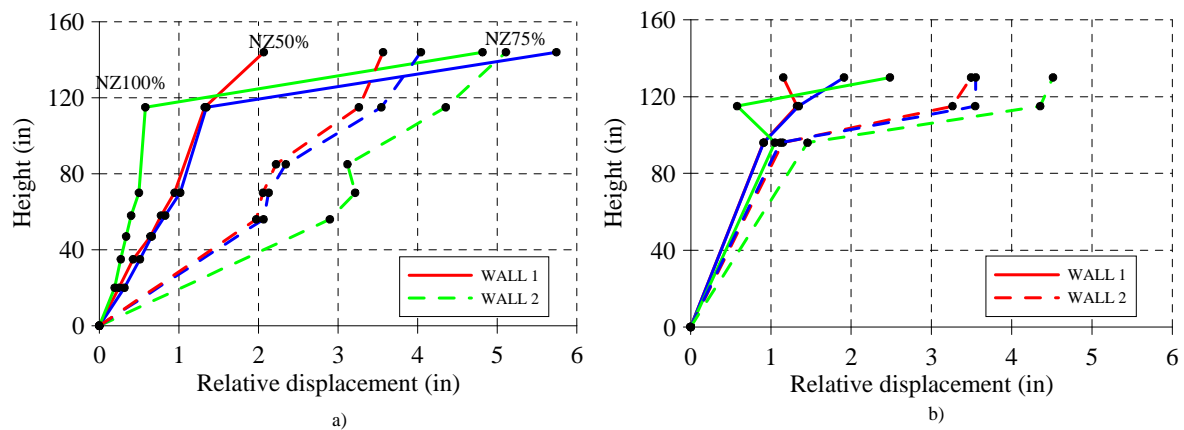


Figure 7. Peak relative displacement profiles of Wall 1 and Wall 2 at a) masonry wall and b) steel tower and isolators

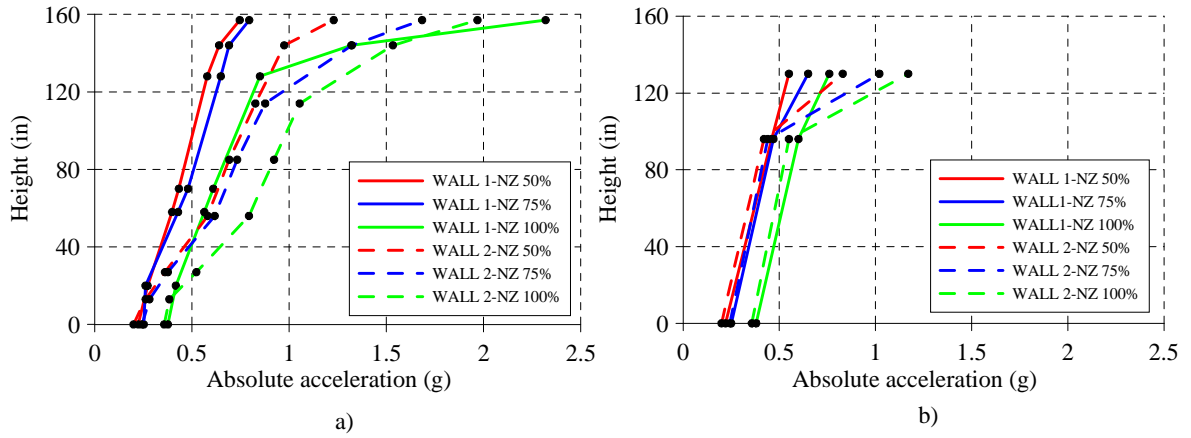


Figure 8. Peak absolute acceleration profiles of Wall 1 and Wall 2 at a) masonry wall and b) steel tower and isolators

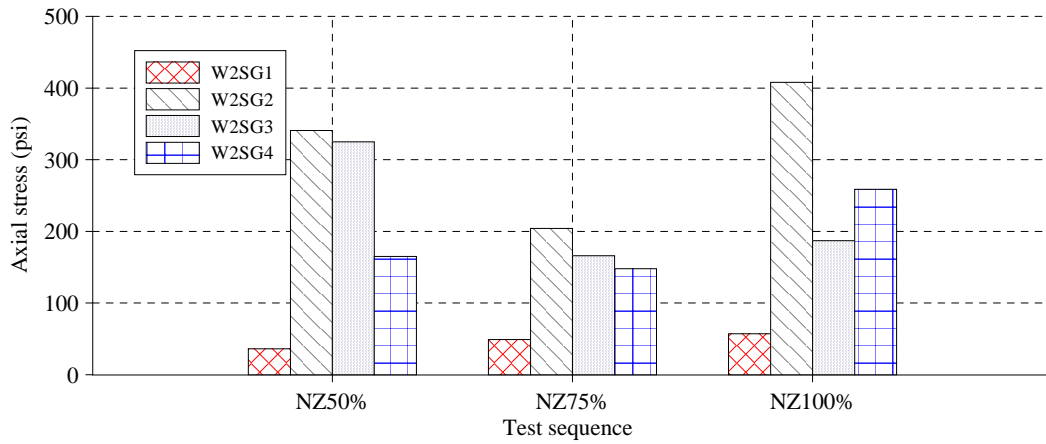


Figure 9. Peak axial stresses in steel anchors of Wall 2

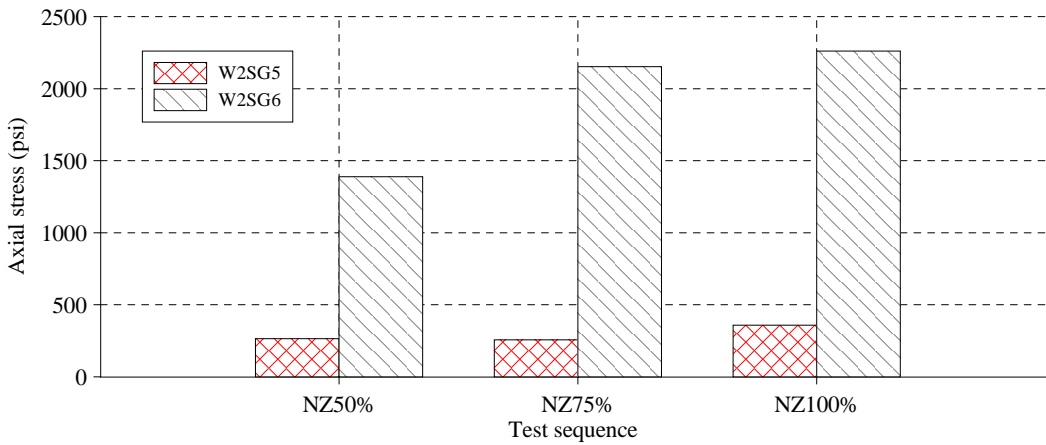


Figure 10. Peak axial stresses in steel braces of Wall 2

HYSTERETIC RESPONSE OF PARAPETS

Data obtained from shake table tests conducted for the more intense ground motions (PGA from 0.22 g to 0.38 g) was used to generate force versus displacement hysteresis loops for the parapets of Wall 1 and Wall 2. The parapet response of Wall 1 is shown in Fig. 11 for all intensity levels of NZ earthquake and the VA300% intensity level. A small relative displacement was obtained for VA300% but the acceleration was still amplified. Moreover, a nonlinear behavior can be observed for intensity levels NZ50% and NZ 75%, which induced large relative displacements and significant amplification of the input acceleration. The parapet collapsed under NZ100%, at time instant $t=2.5$ seconds (See Fig.12a).

For Wall 2 specimen, the nonlinear behavior of the parapet is shown in Fig. 13. After cracking, a predominant frictional and self-centering behavior can be observed at the diaphragm level. Note that for NZ100% large residual deformation were obtained, as seen in Fig. 12b, despite having implemented two standard strengthening techniques.

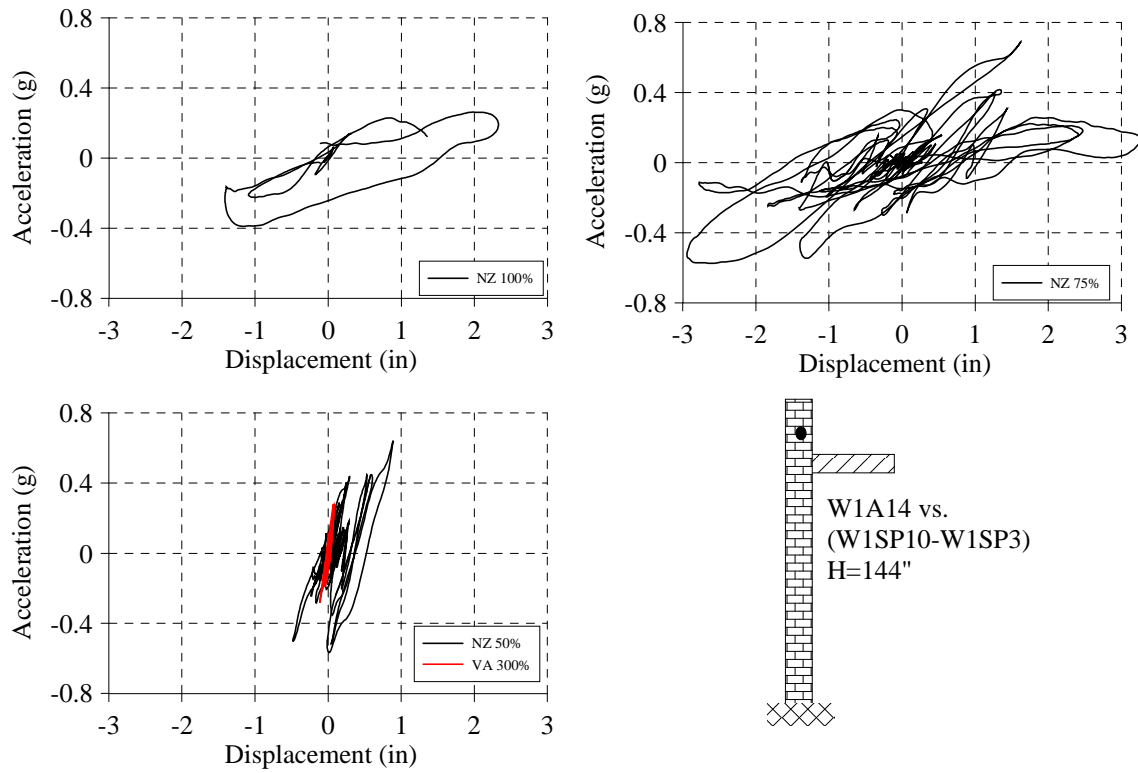


Figure 11. Acceleration versus relative displacement of parapet at Wall 1

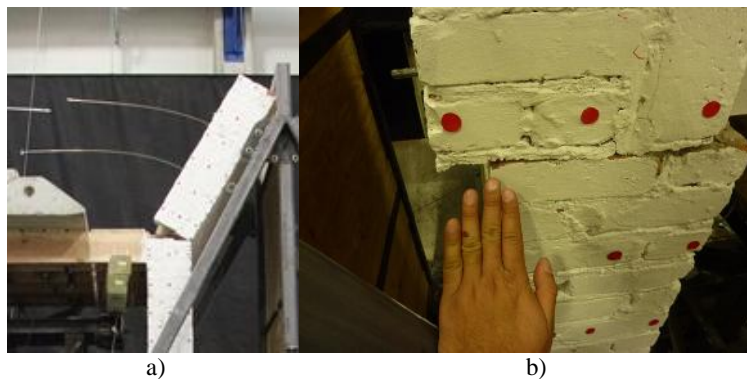


Figure 12. Final damage state of parapets: a) Wall 1 and b) Wall 2

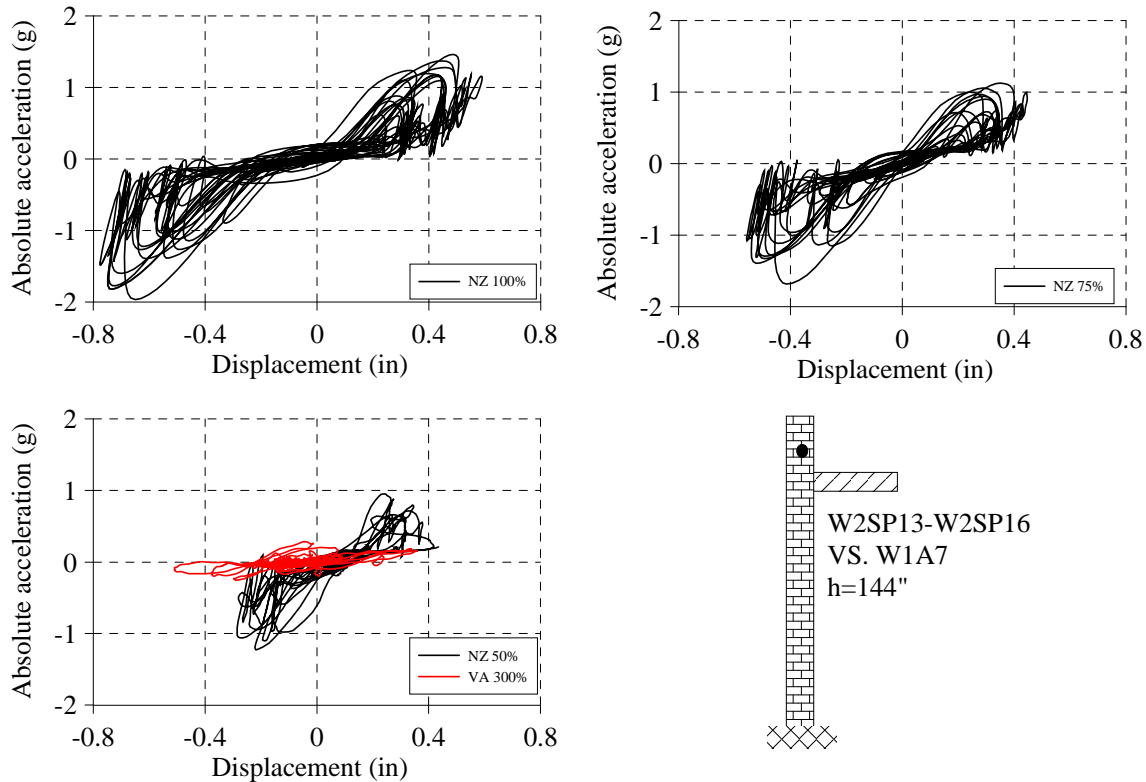


Figure 13. Acceleration versus relative displacement of parapet at Wall 2

CONCLUSIONS

The seismic vulnerability of URM walls with parapets and flexible wood diaphragms to out-of-plane damage and collapse has been experimentally observed.

For low intensity levels of the Virginia Earthquake, no significant differences were observed in the seismic response of walls with flexible and rigid diaphragm. However, the experiments showed that the distribution of the inertial forces, displacements and accelerations in the walls were significantly affected by the presence of parapets and realistic connections in the test setup. Although the specimens were able to sustain the Virginia Earthquake having a PGA of 0.20g with minor damage, the actual vulnerability of full URM buildings in low to medium seismic hazard areas needs to be further investigated.

For strong seismic intensities of the New Zealand Earthquake, common retrofitting techniques were effective in reducing accelerations at the diaphragm and preventing out-of-plane collapse of parapets. However, unexpected failure modes were triggered, thus reducing the overall benefit of the strengthening methods. Numerical studies are under development to understand the impact of several variables (e.g. material properties, diaphragm stiffness, frequency content and duration of the ground motion) in the seismic response of URM walls with parapets and to assess the level of conservatism in the stability limits suggested in ASCE 41.

ACKNOWLEDGEMENT

Financial support for the study described in this paper was provided by MCEER, the State of New York and Arup. The Structural Engineers Association of New York (SEAONY) is collaborating with MCEER on this research project and their support is gratefully acknowledged.

REFERENCES

- ABK (1984). *Methodology for Mitigation of Seismic Hazards in Existing Unreinforced Masonry Buildings : The Methodology*, ABK, El Segundo, Calif.
- Aleman, J. (2014). "Performance-Based Seismic Assessment of Unreinforced Masonry Buildings in New York City." Ph.D. Dissertation, University at Buffalo, Buffalo, NY.
- ASCE 41 (2006). "Seismic Rehabilitation of Existing Buildings ASCE 41-06." American Society of Civil Engineers, 423.
- FEMAP547 (2006). "Techniques for the Seismic Rehabilitation of Existing Buildings." Federal Emergency Management Agency, Washington, D.C.
- Krawinkler, H., Osteraas, J. D., McDonald, B. M., and Hunt, J. P. (2012). "Development of Damage Fragility Functions for URM Chimneys and Parapets." *15 World Conference of Earthquake Engineering*. Lisboa, Portugal.
- Meisl, C. S., Elwood, K. J., and Ventura, C. E. (2007). "Shake table tests on the out-of-plane response of unreinforced masonry walls." *Canadian Journal of Civil Engineering*, 34(11), 1381-1392.
- Penner, O., and Elwood, K. J. (2012). "Experimental Investigation on the Effect of Diaphragm Flexibility on Out-of-Plane Dynamic of Unreinforced Masonry Walls." *15 World Conference of Earthquake Engineering*. Lisboa, Portugal.
- Sanchez-Ferreira, J. (2011). "Stability of Elastomeric Bearings for Seismic Applications." Master of Science, State University of New York at Buffalo, Buffalo, NY.